Design and Testing of a Full Scale Harpoon Capture System

Alastair Wayman[(1)], Andrew Ratcliffe[(1)], Simon Barraclough[(1)], Joshua Lurie[(1)], Ignacio Fernandez-Nunez[(1)], Mihai Lupsa[(1)], Sarmad Aziz[(2)], Kjetil Wormnes[(2)], Martin Zwick[(2)], Nicholas Taylor[(3)], Andy Jardine[(3)], James Campbell[(4)]

[(1)] Airbus, Gunnels Wood Road, Stevenage, SG1 2AS, UK, Email: alastair.wayman@airbus.com
[(2)] ESA/ESTEC, Keplerlaan 1, 2201 AZ Noordwijk, Netherlands, Email: sarmad.aziz@esa.int
[(3)] Cavendish Laboratory, University of Cambridge, JJ Thomson Avenue, Cambridge, CB3 0HE, UK, Email:net20@cam.ac.uk
[(4)]Brunel University London, Kingston Lane, Uxbridge, UK, Email: james.campbell@brunel.ac.uk

ABSTRACT

Active removal of large space debris has been identified as a key activity to control the growth in the debris population and to limit the risk to active satellites. Since 2011 Airbus has been developing a Harpoon capture system to achieve this aim. Since 2015 Airbus has further developed and tested the Harpoon system design as part of the European Space Agency's Cleanspace initiative. Through this, a design able to capture a range of large debris items has been produced, with Envisat and Ariane 4 upper stages used as reference targets. The whole system has been breadboarded and a test campaign begun at full scale in the relevant environment. This paper presents the results to date of the Cleanspace Harpoon project. This includes an overview of the system design, the impact and detumbling simulations performed as well as the results from the test campaign.

1 BACKGROUND

The number of debris objects in orbit is steadily increasing. At present there are over 20,000 catalogued, uncooperative items greater than 10cm in size. Each of these items could severely damage or destroy space assets. For new spacecraft, space debris remediation activities involve post mission disposal alongside manoeuvres through-life to avoid potential collisions. Given the number of objects, the number of collision warnings for operators is increasing as well as the risk of further collisions such as the 2009 Iridium-Cosmos incident. As the number of collisions increases, the debris population will steadily rise until a tipping point is reached where we will see an uncontrollable, exponential growth of debris items which will potentially limit our future utilisation of space.

To reduce the likelihood of an exponential growth in the debris population, Active Debris Removal (ADR) must be considered. Analysis has shown that ADR must remove 5 specific targets per year by 2020 to stabilise the environment [1]. The targets selected are based on their probability of collision and the mass of the target.

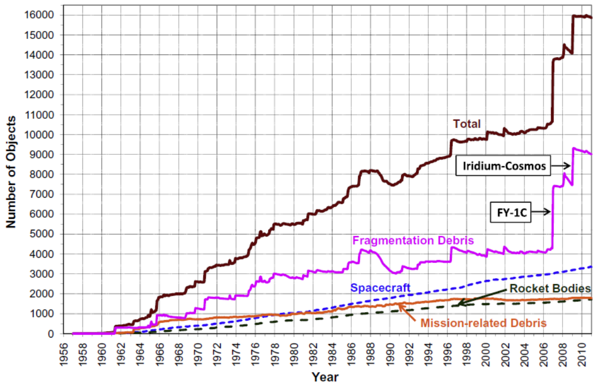

Figure 1. The monthly number of objects greater than 10cm in size in Earth orbit by object type [1]

Upcoming ADR missions involve the launch of a chaser satellite that rendezvous with the target. A key phase of the mission is the target capture. In 2011 Airbus proposed the idea of utilising a harpoon to establish a flexible link with the target. Establishing a flexible link instead of a rigid connection through a robotic arm allows for a stand-off distance to be established, reducing the risk to the chaser during the stabilisation or towing of the spacecraft.

1.1 Initial Harpoon Concept

To progress the harpoon capture technique Airbus has performed internally funded design and breadboarding activities. These activities have proven the basis of the harpoon capture technique under a range of conditions (target and harpoon properties) and have led to the establishment of a baseline Harpoon concept. The original harpoon developed by Airbus is shown in Figure 2. This initial harpoon concept is described in [2].

Proc. 7th European Conference on Space Debris, Darmstadt, Germany, 18–21 April 2017, published by the ESA Space Debris Office
Ed. T. Flohrer & F. Schmitz, (http://spacedebris2017.sdo.esoc.esa.int, June 2017)

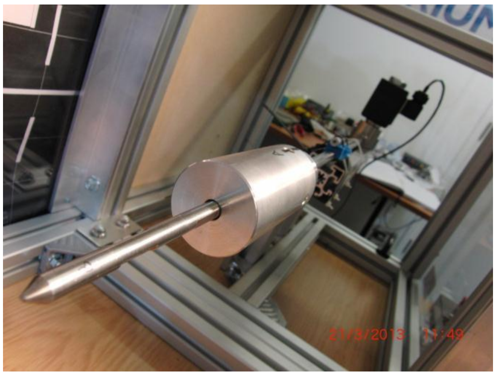

Figure 2. The Airbus R&D harpoon

1.2 RemoveDebris

Following the initial proof of concept, an in-orbit demonstrator of a harpoon system has been developed by Airbus for the European Commission RemoveDebris mission. This mission is scheduled to launch in 2017 to demonstrating several key technologies for active debris removal. The RemoveDebris harpoon experiment will demonstrate the successful capture of a target mounted on a 1.5m deployable boom. The target is a 10cm x 10cm aluminium sandwich panel representative of a small satellite.

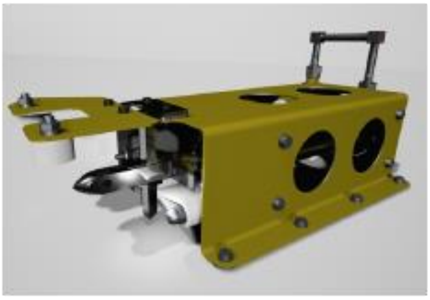

Figure 3. A rendering of the RemoveDebris harpoon system

2 REQUIREMENTS

At the outset of the Cleanspace Harpoon project a set of requirements was defined for the system to be designed against. These requirements covered design, operational, functional, performance, target and environmental requirements. Of these, four can be considered the key driving requirements.

Firstly, the system must be designed to limit the generation of debris both during and after the capture. If pieces of debris are generated, they shall not be larger than 1 mm. The debris risk from the Harpoon system can be split into four categories:

- **Projectile Debris:** Small tear pins within the Projectile are required to fail during the capture. If not contained, these will become debris. As such, the system has been designed to retain all self-generated potential debris
- **Internal Debris:** During the impact, potential debris is generated from the target panel. However, breadboarding activities have shown that this debris is contained internal to the target
- **Fragmentation of the Target:** To prevent fragmentation of the target from the direct impact of the Projectile, the Projectile has a damping system which will limit the penetration distance. Therefore, internal components such as propellant tanks or batteries will not be damaged
- **Free-Flying Projectile:** In the event the Projectile misses the target, it is released to prevent it rebounding and striking the chaser. To mitigate this debris risk, the Projectile has had its radar cross-section increased, allowing it to be tracked from ground

Secondly, the system is required to provide a signal to confirm when a successful capture has been achieved. Ballistic limit testing performed in the context of the study confirmed that the tip diameter has a significant impact on the energy needed to penetrate the target panel. Therefore the challenge is to accommodate the capture confirmation system into as small a volume as possible which is driven by the tip diameter. This capture confirmations system shall instantaneously confirm capture, allowing thrusting to begin. The sensors must also survive the high g-loading associated with impact.

Thirdly, in order to maintain the relevance of the Harpoon system beyond a single mission, the system was required to be sized to capture a range of representative targets. This was taken as at least 50% of the top 30 European targets as defined by the European Mass Weighted (EMW) measure defined in [3]. This measure assesses the risk of each object as a function of its mass, cross-sectional area and the debris flux in its orbit. It includes both satellites and rocket bodies. As such, this will present a different set of target properties that the system must be able to cope with.

Finally, the system shall specifically be capable of capturing an Envisat via an unpopulated panel. This defines the target properties the system must be sized for.

2.1 Target Selection

In order to select the most appropriate target to size the Harpoon system, the top 30 targets from the EMW ranking were grouped by their family; either their satellite bus or their rocket variant. This is shown in Figure 4. From this we can see that 13 of the top 30 targets belong to the SPOT family, where the service module is common between the three generations. This common SPOT service module was used for Envisat.

We can also see that a further 8 of the top 30 targets are Ariane 4 H10 or H10+ upper stages. Again, there is significant commonality between these two variants with the H10+ including stiffening beams along the length of the propellant tanks. This commonality for both the SPOT buses and Ariane 4 upper stages presents a significant opportunity. By designing the Harpoon system for two families of target, it is able to capture 70% of the highest risk European targets, including Envisat, the baseline target and highest risk European object.

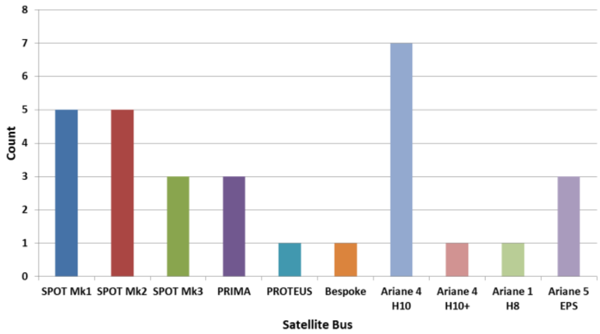

Figure 4. The top 30 EMW targets grouped by family

2.2 Target Properties

In order to capture a target with the Harpoon system, a suitable target area must be found. The accuracy of the Harpoon firing is driven by the size of the areas to be targeted. As such, in order to minimise the requirements placed on the Harpoon system and the chaser, the largest clear area on the target is desired. A detailed assessment of the Envisat mechanical configuration has been performed in order to identify the optimum target locations. An overview of this is shown in Figure 5. At the top of the Payload Module, a significant number of units are housed with thick aluminium baseplates and thermal doublers. There are also a large number of appendages located here. As such, the top of the Payload Module was discarded as a target area. The centre of the Payload Module presents some limited free areas. However, the large ASAR antenna and several large units prevents this from being a preferred target area.

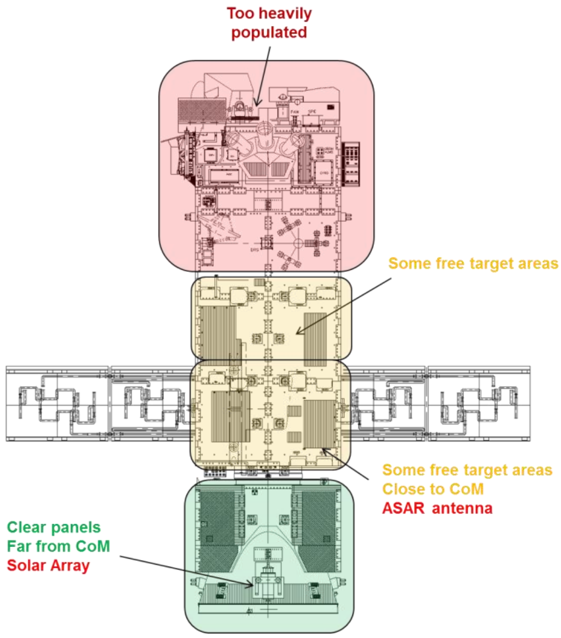

Figure 5. Potential target areas on Envisat for the Harpoon system

On the Service Module there are several panels that are clear of equipment as the units are limited to the +/-Y sides of the module. The +/-Z sides of the Service Module offer the widest areas available for the Projectile impact, with up to a 1m diameter area available. This assists in the relaxing of the Harpoon and chaser targeting accuracy requirements. Additionally, targeting the Service Module also offers the advantage of a structure that is shared by other satellites of interest.

The skins on these panels are 0.4mm thick on the +Z and 1mm thick on the –Z. The honeycomb core is 27mm. Of these two areas, the –Z panel provides a significantly larger target area, as shown in Figure 6 and Figure 7. As such this has been selected as the baseline target area for Envisat.

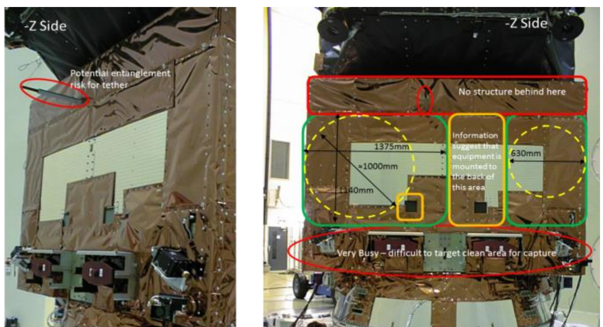

SANDWICH PANEL CHARACTERISTICS

ELEMENT	MATERIAL		THICKNESS (mm)	
	CORE	SKIN	TOTAL	SKIN
SIDE WALL -Z +Y	3/16-.001-5056P	AA 7075 T6	27	1
SIDE WALL -Z -Y	3/16-.001-5056P	AA 7075 T6	27	1

Figure 6. The baseline target area on the –Z panel of the Envisat Service Module

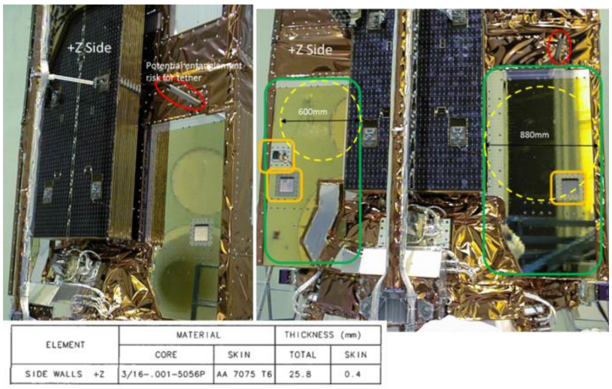

ELEMENT	MATERIAL		THICKNESS (mm)	
	CORE	SKIN	TOTAL	SKIN
SIDE WALLS +Z	3/16-.001-5056P	AA 7075 T6	25.8	0.4

Figure 7. The potential target areas on the +Z panel of the Envisat Service Module

A similar assessment has been performed for the Ariane 4 H10 and H10+. Targeting the propellant tanks directly would provide a large target area significantly simplifying the targeting. However, on the H10+, the internal stiffening beams make targeting this area risky. Additionally, the H10 tanks are a balloon design. This means that without the pressure provided by the propellant, they are flexible, making a successful capture more challenging. As such, targeting the tanks directly was discarded. Targeting the engine nozzle was also discarded as the integrity of it after firing could not be guaranteed. The most promising target area found was the Vehicle Equipment Bay (VEB) at the top of the upper stage. This can be seen highlighted in red in Figure 8.

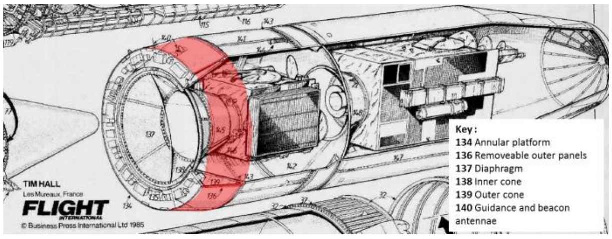

Figure 8. The baseline target area on VEB of the Ariane 4 H10 upper stage

The VEB contains the avionics responsible for controlling the complete launch vehicle during flight. After orbit injection the VEB remains attached to the upper stage. A VEB is shown in Figure 9. Within the VEB an inner cone exists which is attached to the payload adapter. Around the circumference there is a base plate onto which the avionics units are mounted. An outer cone sits between the inner cone and the units. To close the volume occupied by the payloads, a series of closure panels are attached. No units would be mounted to the closure panels by definition. The closure panels are made composite sandwich panels. They are made of 0.36mm thick CFRP skins with a 12mm thick aluminium honeycomb core.

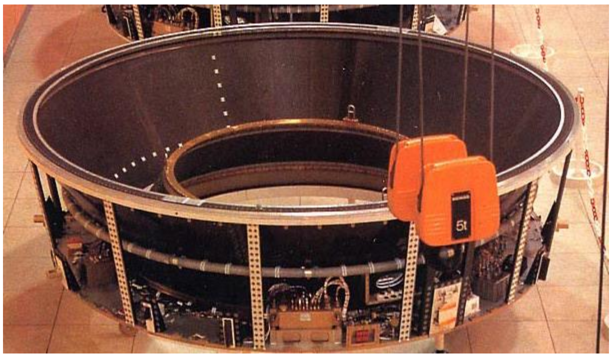

Figure 9. An Ariane 4 VEB with the closure panels removed

3 HARPOON DESIGN

The Harpoon design consists of three key elements; the Deployer, the Projectile and the Equipment Bay. The Deployer restrains the Projectile during launch. Once the target is ready to be captured, it then provides the propulsive force to deploy the Projectile. The Projectile penetrates the target panel and forms the mechanical connection. The two elements are connected by a flexible tether. The equipment bay provides the capture confirmation signal to the chaser spacecraft following a successful capture.

3.1 Deployer

The Deployer uses high pressure gas to accelerate a piston along its length. The Projectile is seated in this piston, and so is similarly accelerated towards the target. An exploded view of the Deployer, highlighting the key functional elements, is shown in Figure 10. The Piston Seat is clamped between the Charge Chamber and the Chamber Union. The Piston Seat and Piston are then connected by a mechanical tear pin creating a rigid assembly. At this point, the piston is sat within the Chamber Union between Plenum A and Plenum B. Before firing, Plenums A and B are charged to the firing pressure. This pressure will provide the main propulsive force for the Projectile, but is currently acting only on the sides of the piston. When ready to fire, the Charge Chamber is pressurised. The Piston Seat has a series of holes in it, allowing pressure to build on the rear of the piston putting the Tear Pin into tension. Once sufficient pressure is reached, the Tear Pin will fail and the Piston will begin to accelerate forward. This will open Plenums A and B, allowing their high pressure gas to act on the rear of the piston, accelerating it rapidly along the length of the Barrel. A rubber End Stop at the end of the barrel prevents the Piston from being damaged. A set of holes around the circumference of the Barrel allows the high pressure gas to vent from behind the Piston after firing.

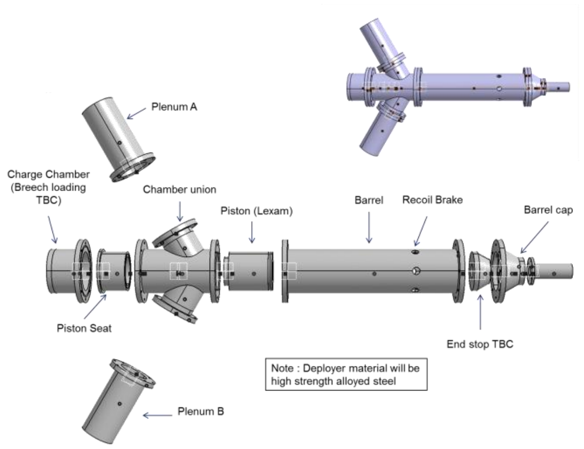

Figure 10. The functional elements of the Harpoon Deployer

The design of the Deployer is highly flexible. It is able to accelerate the Projectile to a wide range of speeds. No mechanical change is required for this, simply a change in the pressure in Plenums A and B. The system is sized to operate from 4 to 80 bar. Approximately 25 bar is required for the baseline target panel.

3.2 Projectile

The Projectile is a complex and highly integrated element of the Harpoon system. It is approximately 1m in length and has a mass of 2.2kg. Its primary function is to penetrate the target and form a reliable mechanical link. The operational sequence of the Projectile is shown in Figure 11. This goes from deployment, through penetration and barb release to capture and detumbling.

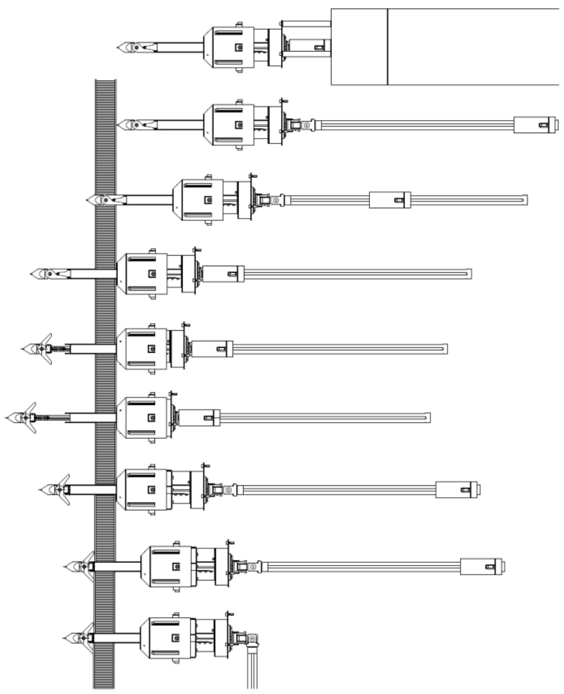

Figure 11. The Projectile sequence of operations

Upon contact with the target the ogive Tip of the Projectile locally deforms the target panel. A sharp point on the front end of the Tip is used to create a pilot hole upon contact. This feature reduces risk that the Projectile will slide along the panel or bounce away at high incidence angles.

The Projectile penetrates through the panel, driven by its momentum until it has travelled a sufficient distance to impact the Collar. The profile of the Tip Assembly and Collar is constant (or as near as can be), with all parts and features (barbs, pin heads, hold downs) flush or sub-flush with the Tip. This design supports smooth travel through the Target panel, with reduced risk of snagging or jamming during penetration and subsequently during pull-back of the Collar due to tether loads.

Once the Collar's conical 'impact plate' encounters the target this provides the force needed to cause failure of the Barb Lock Pins. At this point the spring loaded Upper Barb pair deploys inside the panel. Their release allows the similarly spring loaded Lower Barb pair to deploy. This creates the mechanical linkage with the Target. Each individual barb has been sized to support the peak load to account for the possible eventuality that only a single barb could be in contact with the panel.

The length of the Tip shaft and Collar has been driven by the 45° incidence angle case, and has been sized so that there is sufficient clearance for both sets of barbs to deploy, with margin, above the panel surface and above several millimetres of potential petalling.

The Projectile features an energy absorption device in the form of a crushable honeycomb cartridge. The purpose of this device is to sink additional excess kinetic energy which could lead to damage to the target panel, generating debris or degrading the mechanical link. This was originally sized to absorb the difference in energy between a normal impact and a 45º impact. A normal impact would have additional energy after penetration due to the lower ballistic limit.

As well as form the mechanical link to the target, the Projectile must also attach to the tether. This is done through an attachment that is able to both slide and rotate. For flight stability purposes, application of the tether drag force should be as far behind the Projectile centre of mass as possible. The tether attachment should ideally be located at the end of the Shaft. However, accommodation of such an attachment is constrained by both the Deployer (Barrel volume, Barrel Cap) and routing of the tether when stowed during launch and prior to deployment. The approach taken is for the tether attachment point to be located outside of the Deployer but able to travel linearly along the shaft until it reaches an end stop. Sliding is achieved via the Tether Slide, which interfaces with a groove pattern within the End Shaft. The tether is enabled to rotate both to prevent imparted moments on the Projectile during deployment and to reduce the risk of tangling due to the motion of the target relative to the chaser after capture. This rotation is enabled by the Tether Swivel.

Figure 12. The Cleanspace Harpoon Projectiles with their barbs deployed

The Projectile has been designed to survive the loads experienced during operations. The key drivers for the loads are the deployment, the penetration and the detumbling. The peak load seen by the Projectile during deployment with an 80 bar pressure in Plenums A and B is approximately 22kN. Given the increase in mass of the Projectile over the life of the project, a pressure closer to 25 bar is required for an Envisat like panel. As a consequence, the Projectile has been oversized for a flight representative case. During the penetration, the peak loads expected are of this order. This narrow separation presents a challenge for the design of tear pins. These are required to not fail during deployment, but fail during impact. However, as previously stated, the 80 bar maximum firing pressure is no longer a representative case. During the detumbling, the Projectile End Shaft will extend out of the target panel by c.0.5m. As the target rotates, this will lead to a significant moment arm, driving the size and mass of the End Shaft to an unfeasible size. To counter this, a Universal Joint has been included at the top of the End Shaft. Two tear pins hold this in place during deployment. These then fail once a lateral load is applied to them, allowing the End Shaft to lay parallel to the target panel surface if required. Two full projectiles have been procured for the test campaign. They can be seen assembled in Figure 12.

3.3 Equipment Bay

The Equipment Bay is located towards the middle of the Projectile. Its function is to provide a signal to the chaser confirming a successful capture has occurred. The capture is confirmed in two ways.

Firstly, the release of the barbs is detected. One micro-switch is placed underneath each of the Lower Barbs, with the switch plunger engaged when the barbs are held down and released when the barbs are released. The need for switches under the Upper Barbs was deemed unnecessary since the Lower Barbs are only able to deploy if the Upper Barbs have already deployed.

Ideally, the switches would be able to detect when the barbs have travelled fully to their end stops rather than detection of their initial release. Implementation of this was assessed but due to the limited volume available within the Tip sub-assembly (driven by limited cross-sectional area) it was not possible to facilitate this.

Secondly, the acceleration of the Projectile through the panel is measured. For sandwich panels as used on most spacecraft, a double peak of acceleration will be seen for a successful capture; one peak for each skin. If this profile is seen, a penetration can be inferred.

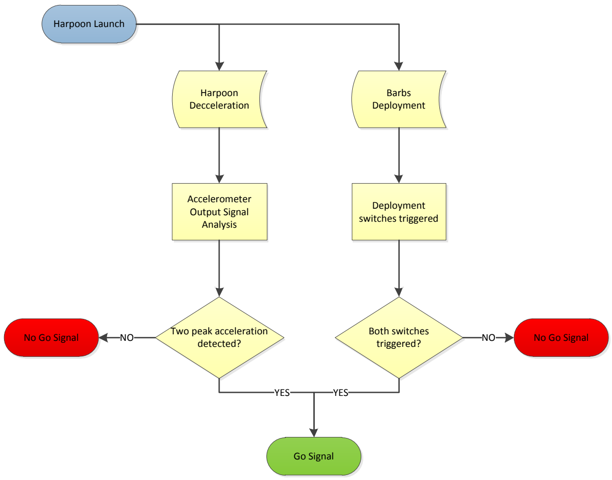

Figure 13. The capture confirmation sequence

The micro-switch and accelerometer signals are fed into an on-board processing unit, which performs the checks required to make an assessment of target capture. This processor is then able to transmit the confirmation signal via a transmitter within the Equipment Bay. The sequence for the capture confirmation is shown in Figure 13.

4 IMPACT TESTING

In order to inform the design of the tip geometry, a series of tests were performed to determine the ballistic limit of different tip designs. These were performed using a gas gun at the Cavendish Laboratory, Cambridge. The set-up is shown in Figure 14. A 125mm square target panel was held down by four fasteners, one in each corner. A free flying 150g projectile was fired at the target. The impacts were recorded and the residual velocity calculated for each. The ballistic limit was then calculated from this using the simplified perforation model of Recht and Ipson (RI) [4].

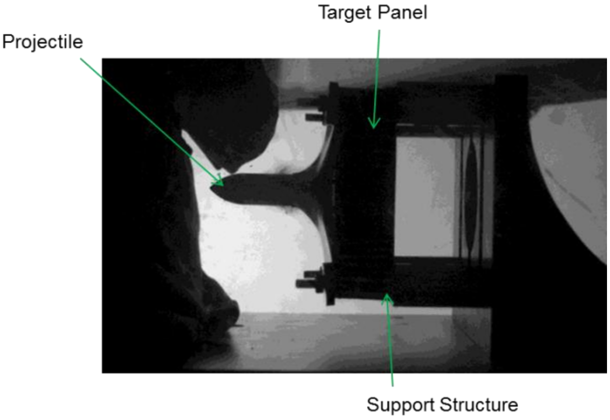

Figure 14. The test set-up for the ballistic limit tests

A series of 6 different projectile types were used, including three nose-shapes and two rod-diameters. The nose-shapes included an ogive of sharpness 1.5, a 60° cone, and a flat end, each with diameters of 10 mm and 20 mm. The ballistic limit for each of these was determined for a normal incidence. Additionally, the ballistic limit for a 45° incidence angle was determined for the 20mm tips.

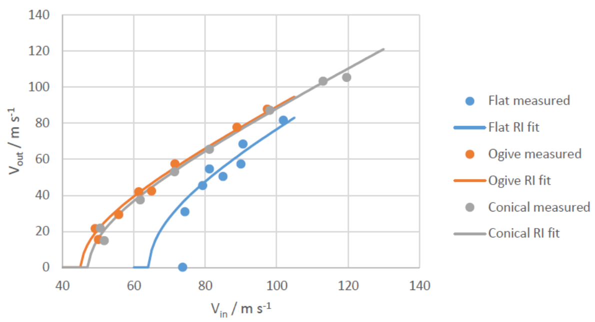

Figure 15. A comparison of residual velocities with varying projectile shape for 20 mm projectiles at normal incidence

The results of tests for the 20mm tips are shown in Figure 15 for a normal incidence and Figure 16 for a 45° incidence. From these we can see that the performance of the flat tip is significantly worse than the conical and ogive tips at normal incidence. As such, it was discarded. At high incidence angles the performance of the three geometries is very similar. The ogive tip appears to hold a slight advantage as the ballistic limit is approached. However, this advantage is minimal. Because of this, the ogive tip was selected as the baseline; however the use of the conical tip is also valid.

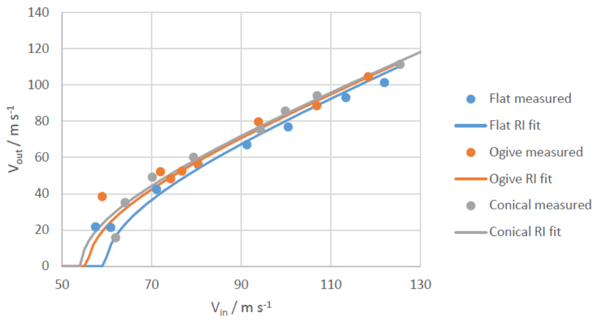

Figure 16. A comparison of residual velocities with varying projectile shape for 20 mm projectiles at 45° incidence

5 IMPACT SIMULATIONS

Following the impact testing performed, simulations of the impact were also performed. The objectives of these were to:

- Model the impact experiments with the 150g projectile to validate the modelling approach
- Model an impact on a larger panel to investigate the influence of structural flexibility
- Model the impact on the larger panel with a 1.59kg, representative Projectile and determine the ballistic limit

The models were run over a series of impact angles and impact velocities as shown in Table 1.

Target	Projectile	Impact angle	Impact Velocity (m/s)						
Experimental panel	Experimental	0°	70	60	55	48			
		45°	93	80	74	60			
Large panel	Experimental	0°	70	60	55	48			
		45°	93	80	74	60			
	Representative	0°	55	48	40	30	-	20	17
		45°	74	60	40	30	25	20	-
		22.5°	-	60	40	30	25	20	-

Table 1. The analysed impact conditions

The experimental panel is shown in Figure 17. The skins were modelled using 207,840 solid elements per sheet. The honeycomb core was modelled using 378,160 shell elements. The projectile and panel supports were assumed to be rigid. A sensitivity study using the 0°, 70m/s, impact condition was used to determine appropriate assumptions for the model, including the coefficient of friction between the projectile and the panel as well as the strength and ductility of the face sheets. These properties all had a strong influence on the model results. A coefficient of 0.47 was initially used, however this resulted in the projectile failing to fully penetrate the panel. A coefficient of 0.1 was found to be the highest value consistent with a reasonable exit velocity. The strength and ductility of the face sheets needed to be reduced for the model results to match the experimental results.

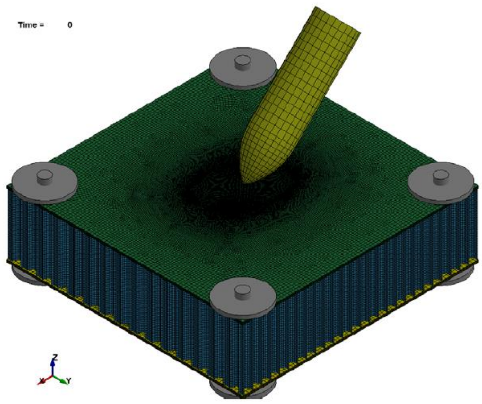

Figure 17. The modelled experimental panel modelling

Following the sensitivity analysis, the model was updated and re-run over a range of impact velocities from 44m/s to 98m/s. No changes beyond the impact velocity were made between the simulations. The results of these are compared to both the experimental results and the RI model in Figure 18. The case used for the sensitivity analysis is highlighted by a black diamond. From this we can see that there is strong agreement between the simulation, experimental and RI model results over the whole range of velocities considered, validating the modelling approach.

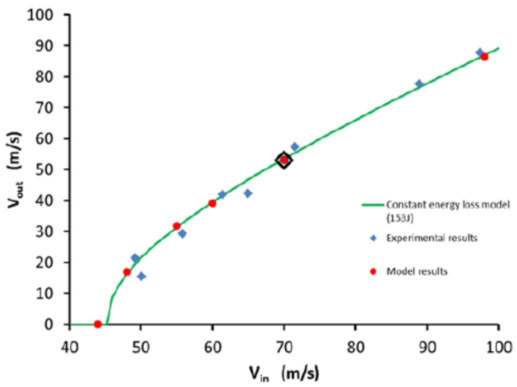

Figure 18. The experimental panel modelling results for a normal impact

With the modelling approach validated, the large panel representative of the physical target panel was modelled along with a representative Projectile. These can be seen in Figure 19. For this, a central section based on the experimental panel was modelled in detail with the remainder of the panel modelled at lower detail to reduce the computational cost to a reasonable level. The size of the central section was determined by the extent of deformation in the experimental models. Simulations were performed with both the 150g experimental projectile and the representative 1.59kg Projectile. This consisted of a detailed model of the ogive tip transitioning to a square section. The remainder of the Projectile was included to aid visualisation.

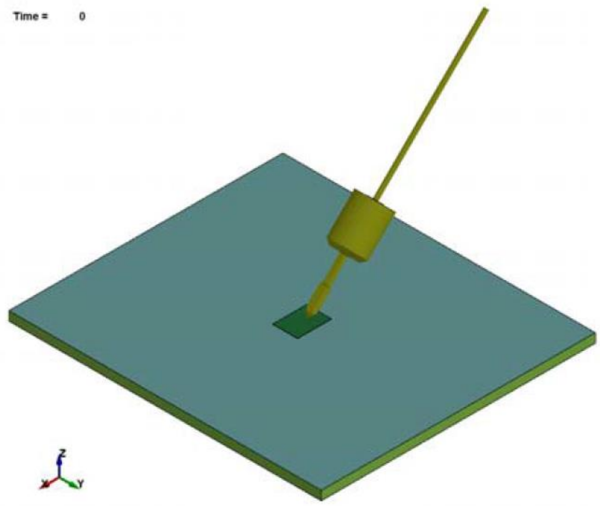

Figure 19. The set-up for the large panel modelling

A total of seventeen analyses were completed with the representative Projectile: six 0º, five 22.5º and six 45º covering impact velocities between 17m/s and 74m/s. These are shown in Table 1. The 45º impact drives the ballistic limit, with the results shown in Figure 20. From this we can see the ballistic limit is approximately 20m/s. Again, the simulation results agree with the RI model well.

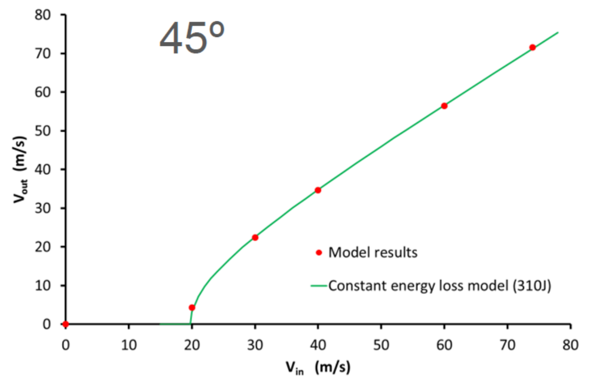

Figure 20. The results of the large panel modelling for an impact angle of 45 degrees

As a secondary output of the simulations, the acceleration profile of the Projectile as it penetrates the panel was produced. This was a beneficial input to the design of the Equipment Bay. The acceleration profiles for a 45º impact over a range of impact velocities are shown in Figure 21. From these we can see the characteristic double peak that will be used as one of the capture confirmation signal inputs. We can also see that the magnitude of the acceleration is only weakly dependent on the impact velocity, decreasing by less than 10% for a reduction in impact velocity by a factor of almost 3.5. The time between the peaks is inversely proportional to the impact velocity, as is expected.

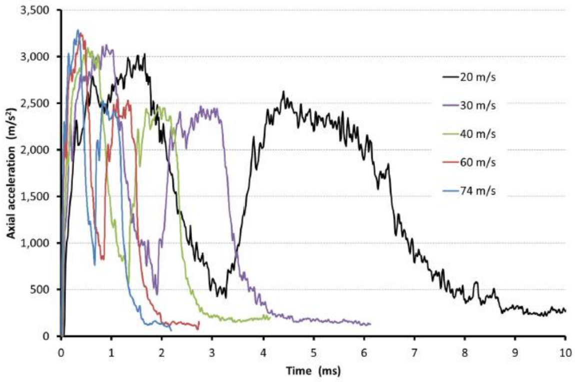

Figure 21. The Projectile acceleration as a function of time for the large panel modelling with an impact angle of 45 degrees

6 DYNAMIC MODELLING

Following the successful capture, a tether will be used to transfer the detumbling and towing loads from the chaser to the target. In order to assess these loads, a dynamic analysis of the target and chaser after capture was performed. This analysis used a combination of MSC ADAMS and the Airbus developed dynamics tool DYCEMO. The analysis was performed for Envisat, an Ariane 4 upper stage and MetOp. A visualisation of the dynamics model can be seen in Figure 22.

The multibody dynamics is realised via two independent rigid plants (i.e. the chaser and target) with a single, massless ‘slack spring’ tether model with both stiffness and damping modelled in the axial direction. The tether interface is modelled as a frictionless ball joint at both ends. This represents a simplification of a full 6DoF multiple mass linked tether model. This was done in order to facilitate a large number of simulations for Monte-Carlo style runs. A comparison was made between a multiple-mass-in-series model and the massless single slack spring model which confirmed the fundamental behaviour was equivalent, thereby proving the suitability of the simplified model for the current analysis.

Initially a constant thrust model was assumed, with the thrust initiated as soon as the capture confirmation signal was received. This led to a large snatch load of up to 8kN as the chaser had a large velocity relative to the target as the tether went into tension. This was mitigated by allowing the rotation of the target or a short period of thrust once the capture confirmation signal is received to bring the tether into tension. The thrust was then triggered as the tether went into tension, eliminating the relative velocity between the target and chaser. Following this approach, the peak load was reduced to below 1.8kN for the three targets analysed. The results for the Envisat Monte Carlo analysis are shown in Figure 23. A thrust of 500N along the initial tether direction was assumed.

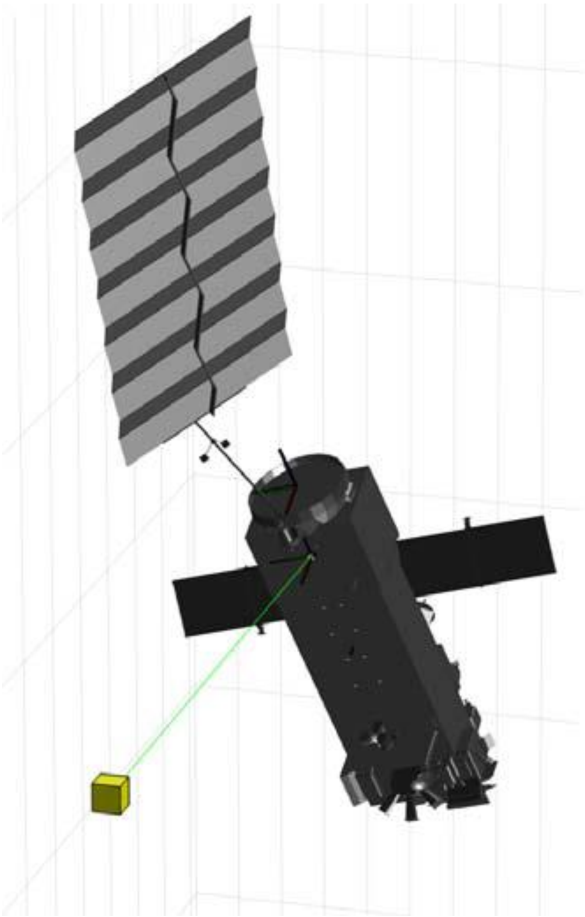

Figure 22. The dynamics model 3D visualisation

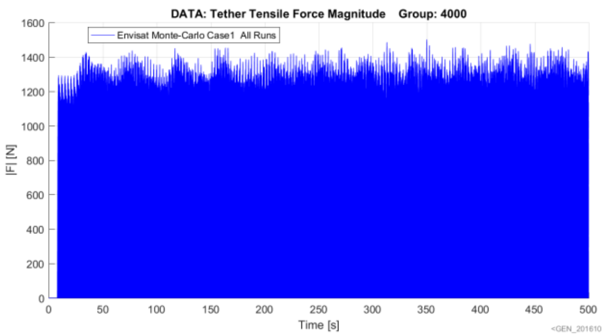

Figure 23. The tether tension as a function of time for the detumbling of Envisat

With these loads defined, the Envisat Finite Element Model was used to confirm the target panel could sustain them. It was confirmed no cleats would fail and the panel would survive the loads.

7 CHARACTERISATION TESTING

The activities described so far have resulted in the design of the Harpoon system. As part of the Cleanspace Harpoon project, the system has been breadboarded and a bespoke test rig produced. This will allow the system to be fully characterised through a dedicated test plan. This will culminate in a series of full scale test over the full firing distance, validating the system and achieving TRL5. This testing is scheduled to complete by the end of summer 2017. The test plan has been designed to characterise all aspects of the system and verify all of the requirements have been met. In total, 131 individual tests are anticipated.

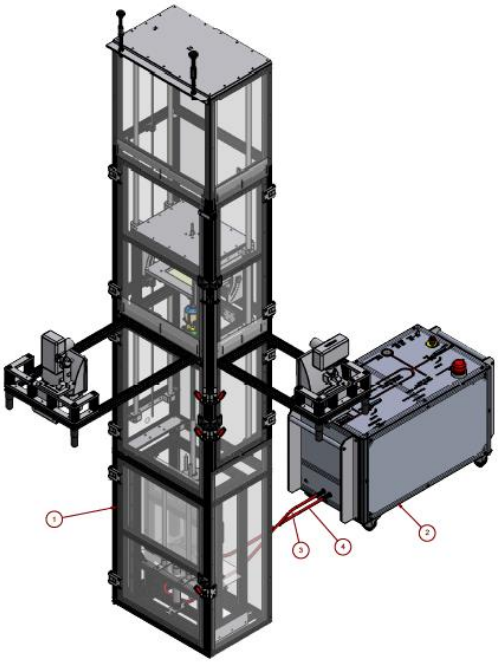

Figure 24. A model of the Cleanspace Harpoon test rig

A model of the test rig used for the majority of the testing can be seen in Figure 24. The physical test rig can be seen in Figure 25. The Deployer is located at the base with the Projectile fired vertically up. This removes the effect of gravity on the trajectory with the velocity lost compensated for by an increased firing pressure. The target is located on a movable carriage that can be located in two locations, allowing tests over distances of approximately 1m and 2m respectively. The carriage is locked in place before each test, with the target clamped around its edges by a ‘picture frame’. The target can be rotated, allowing tests at incidence angles between normal and 45º. High speed cameras are used to record the deployment and impact. A pressure transducer is used to record the pressure during the deployment and a speed trap is used to measure the deployment speed.

Figure 25. The physical Cleanspace Harpoon test rig

To date, initial tests have been performed demonstrating the test equipment and procedures as well as the key functionalities of the Harpoon system. The Deployer has been shown to successfully hold pressure until required to deploy the Projectile. It has also been demonstrated to successfully deploy the Projectile by breaking the piston tear pin at the expected pressure. The Projectile has been shown to successfully penetrate a representative target panel with the Barbs successfully deployed and the Universal Joint remaining locked until after impact. Images of the Projectile following a test can be seen in Figure 26 and Figure 27. With these basic functionalities demonstrated, further quantitative testing will be performed as through the test campaign.

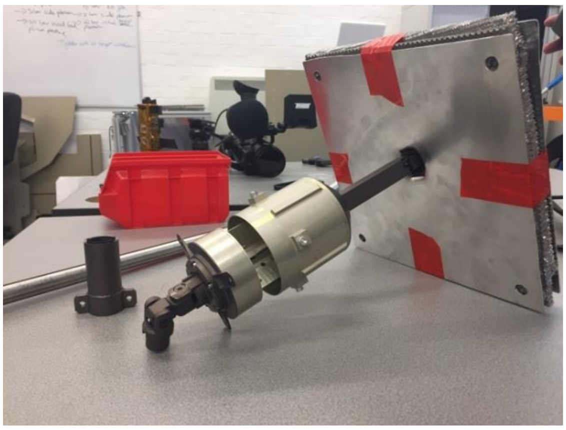

Figure 26. The Projectile embedded in a test panel after firing. The panel has been removed from the test rig and the end shaft removed from the Projectile

Figure 27. The Projectile embedded in a test panel after firing

8 CONCLUSION

A set of requirements for a Harpoon capture system have been defined considering a range of targets. Based on these, a complete Harpoon system has been designed, comprising three key elements; Deployer, Projectile and Equipment Bay. The design has been informed by a set of impact tests and associated simulations. Appropriate margins have been applied leading to a robust design. This has led to a design that is flexible and scalable to a wide range of targets. The loads seen during the detumbling and towing have been determined through simulations, and the survivability of the Envisat target panel confirmed. The system has been designed to prevent the generation of any secondary debris. The inclusion of a capture confirmation signal provides further robustness to the system and operational concept. The Harpoon system has been breadboarded and a test plan produced to characterise and validate the system. To date, the basic functionalities of the Harpoon system have been demonstrated, giving confidence in the concept and the design. The test campaign will culminate with a set of full scale, end-to-end validation tests in summer 2017. These will raise the Harpoon system to TRL5.

9 REFERENCES

1. Liou, J.-C. (2011). An Active Debris Removal Parametric Study for LEO Environmental Remediation. *Advances in Space Research*. **47**, 1865-1876

2. Reed, J. & Barraclough, S. (2013). Development of Harpoon System for Capturing Space Debris. In *Proc. 6th European Conference on Space Debris* (Ed. L. Ouwehand)ESA Sp-732(ISBN 978-92-9221-287-2) ESA Publications Division, European Space Agency, Noordwijk, The Netherlands.

3. Möckel, M. et al,. (2010). Orbital Debris Removal – Priority List. *Technical Report.*

4. Recht, R. & Ipson, T.W. (1963). Ballistic Perforation Dynamics, *Journal of Applied Mechanics*, **30**(3), 384-390